EXPERIMENTAL TEST SET-UP FOR STUDYING HOT CRACKING IN MULTI PASS LASER HYBRID WELDING OF THICK SECTION AUSTENITIC STAINLESS STEEL

Paper 1203

Miikka Karhu[1] and Veli Kujanpää[1,2]

[1]VTT- Technical Research Centre of Finland, P.O. Box 17021, FI-53851 Lappeenranta, Finland
[2]Lappeenranta University of Technology, P.O. Box 20, FI-53851 Lappeenranta, Finland

Abstract

Although the austenitic stainless steel grades are commonly considered to be quite easily weldable, there are certain applications which make exception to the above statement. As an example, which has also attributed to this study, it could be mentioned a welded assembly which forms a very rigid structure. In above mentioned structure, a risk of solidification cracking (i.e. hot cracking) in produced welds could be a significant problem, if necessary precautions are not taken into account well in advance. It is generally known that hot cracking of austenitic stainless steel during welding is very much coupled to chemical composition and the strains formed during solidification stage of the weld. The level of strains is dependent on e.g. a groove design, used welding parameters and the rigidity of the structure to be welded. In this work the main objective was to find a method for studying hot cracking susceptibility when a thick section austenitic stainless steel is welded using laser hybrid welding process (3 kW Nd:YAG-laser + GMAW) and multi pass technique. The tested parent material was a specially customized heat: AISI 316L(N)-IG ITER-grade austenitic stainless steel. During this study the test system was first developed and tested. It consists of a very rigid clamping system and specially designed 60 mm thick test piece which was planned to be rigid as itself. The test welds were evaluated with macroscopic and microscopic examination. In addition NDT was used as well. The results of welding tests showed that the developed test set-up can produce strains high enough to promote hot cracking in produced test welds. According to welding test results, hot cracking occurred in these rigid weld arrangements. The test set-up is described and the results of hot cracking tests are reported. The effect of chemical composition of the used parent/filler material and prevailing micro structure of weld metal on the risk of hot cracking susceptibility is discussed as well.

Introduction

Various constitutional diagrams have been developed in order to evaluate a weldability of stainless steels [1,2,3,4]. For example, the use of those diagrams could help to predict as-welded microstructure and avoid unfavourable parent material or filler material compositions which could lead e.g. to solidification mode or microstructure favouring hot cracking. The diagrams are based on chromium (Cr_{eq}) and nickel (Ni_{eq}) equivalents and their ratio (Cr_{eq}/Ni_{eq}) which can be calculated when a chemical composition of parent material and filler material is available. In the case of conventional arc welding where solidification rate is slow, it is found that if the ratio of chromium and nickel equivalent (Cr_{eq}/Ni_{eq}) in weld metal is below a certain level, e.g. 1.5, the susceptibility for solidification cracking is much higher than in welds where chromium and nickel equivalent ratio is above 1.5. The critical ratio is depending on the solidification rate such that at the higher solidification rates the critical ratio is slightly increased. This is observed to be case e.g. in laser or electron beam welding. The impurities, especially sulphur and phosphorus also play a role in the susceptibility of hot cracking. If the impurity content is very low, below 0.01 %, the susceptibility is much decreased, [5,6,7,8,9,10].

The hot cracking susceptibility is also dependent on the level of strains affected by the rigidity of the structure. If the structure is very rigid, the strains causing hot cracking develop much easier. Furthermore, it is commonly recognized that in applications, where fully austenitic stainless steel welds are in certain specific reason required (e.g. anti-magnetic requirements etc.), hot cracking in weld metals could cause remarkable problems.

For the above reasons the ordinary austenitic stainless steel composition is often balanced such that usually ordinary AISI 316L or AISI 316LN composition is on the safe composition range, i.e. the ratio of chromium and nickel equivalents is over 1.5, which should ensure

that solidification is primary ferritic resulting in approx. 5 to 15 % delta ferrite in the weld metal at room temperature. This has been observed to prohibit hot cracking. Another import factor for hot cracking prevention is reduction of impurity content (S+P); for safety reason it is usually limited to 0.03 … 0.04 %.

The scope of this study is related to research area, where new high efficiency joining possibilities for an assembly of very massive thick section vacuum vessel, made out of austenitic stainless steel, were explored. Considering the assembly phase of above mentioned vacuum vessel, if hot cracking occurs, it could be highly detrimental, because minor hot cracks cannot be revealed during welding, but only later in NDT inspections, in the worst case long time after the whole weld is finished. This could cause laborious and time-consuming repair procedure with additional costs and delay of the work. Repair welding may also be very harmful with regard to welding distortion control. Therefore it is extremely important to avoid hot cracking as complete as possible.

The ratio of chromium and nickel equivalents in used vacuum vessel material ITER grade austenitic stainless steel AISI 316L(N)-IG was calculated according Hammar & Svensson equitions (Ref. 4). Calculations revealed that depending on the variation of the element contents, Cr_{eq}/Ni_{eq} -ratio is in the range of 1.2 to 1.5, which marks risk of hot cracking. In the tests of basic AISI 304L and AISI 316LN laser and hybrid laser multi pass tests, clear indication of hot cracking was seen in many test welds. Therefore it may well be judged that AISI 316L(N)-IG ITER steel grade is susceptible to hot cracking, if other conditions favouring hot cracking, e.g. high rigidity of joint, fully austenitic as-welded microstructure etc. are present.

Stem from above mentioned aspects, a hot cracking study was conducted. The purpose of this study was to develop a test set-up for studying hot cracking in multi pass laser hybrid welding of thick section austenitic stainless steel and then use this set-up for evaluation of hot cracking susceptibility of welds produced into the special customized heat AISI 316L(N)-IG ITER-grade by using certain reference filler wire material (THERMANIT 19/15). The concept of the test set-up was to use a straight forward approach in designing; A very rigid clamping table together with fastening system and a test piece-design which is very rigid it self and produces self restraint was built.

Experimental Procedure

Materials

Parent material used in the experiments was a specially customized heat AISI 316L(N)-IG ITER-grade austenitic stainless steel. Filler wire used in the experiments was an austenitic stainless steel wire THERMANIT 19/15 with a diameter of 1,2 mm. The chemical compositions of the materials are shown in Table 1 and 2, respectively.

Table 1. Chemical composition of the parent material AISI 316L(N)-IG according to EN 10204-3.1B.

Parent material	**Chemical Composition (wt%)**			
AISI 316L(N)-IG	**C**	**Mn**	**Si**	**P**
	0,025	1,7	0,36	0,021
	S	**Cr**	**Ni**	**Mo**
	0,0001	17,6	12,2	2,41
	Ti	**Ta**	**Nb**	**Cu**
	0,005	0,003	0,005	0,1
	B	**Co**	**N**	
	0,0004	0,03	0,067	

Table 2. Chemical composition of the filler wire THERMANIT 19/15 according to EN 10204-3.1B.

Filler wire	**Elemental Composition (wt%)**			
THER-MANIT 19/15	**C**	**Mn**	**Si**	**P**
	0,015	7,32	0,46	0,013
	S	**Cr**	**Ni**	**Mo**
	0,005	20,18	15,08	2,79
	Cu	**Co**	**N**	
	0,095	0,016	0,187	

Welding equipment

Welding experiments were performed by using a combination of Nd:YAG-laser process and MIG-process. The laser used in hybrid process was HAAS-LASER GmbH model HL 3006 D with Ø 0,6 mm optical fiber beam delivery system, Figure 1. The laser has a maximum output power of 3 kW at the surface of a work piece. The full power of 3 kW was used in all experiments. Used lens focusing optic gives a 200 mm focal length, 6,12 degree focusing angle and can provide a spot diameter of 0,6 mm in the focal point. The laser system enables a beam parameter product of 25 mm·mrad. GMAW machine used in the hybrid welding was KEMPPI Pro 5200 equipped with ProMIG 501 unit, Figure 1. KUKA KR 15 robot was used in order to execute required welding movements. Self tailored hybrid welding head was mounted in the wrist flange of KUKA-robot, Figure 1.

Figure 1. Welding equipment used in the experiments. On the top: 3 kW Nd:YAG-laser, On the left: Kemppi Pro MIG-welding machine, On the right: Hybrid welding head mounted in KUKA KR 15 robot.

Hot Cracking Test Set-Up: Rigid clamping table and test piece design

A very rigid clamping system was designed and built in order to emulate rigid welding conditions and strains which can occur in massive components assembly welding. The test system consists of rigid 170 mm thick table and clamping system for that, Fig. 2. In clamping system, the total of 6 pieces of Ø 30 mm diameter high strength bolts together with 40 mm thick holder blocks was used to minimize angular distortions caused by welding heat. Each bolt was tightened into the moment of 1500 Nm with using dial torque wrench. That equals approx. a 300 kN compression per bolt.

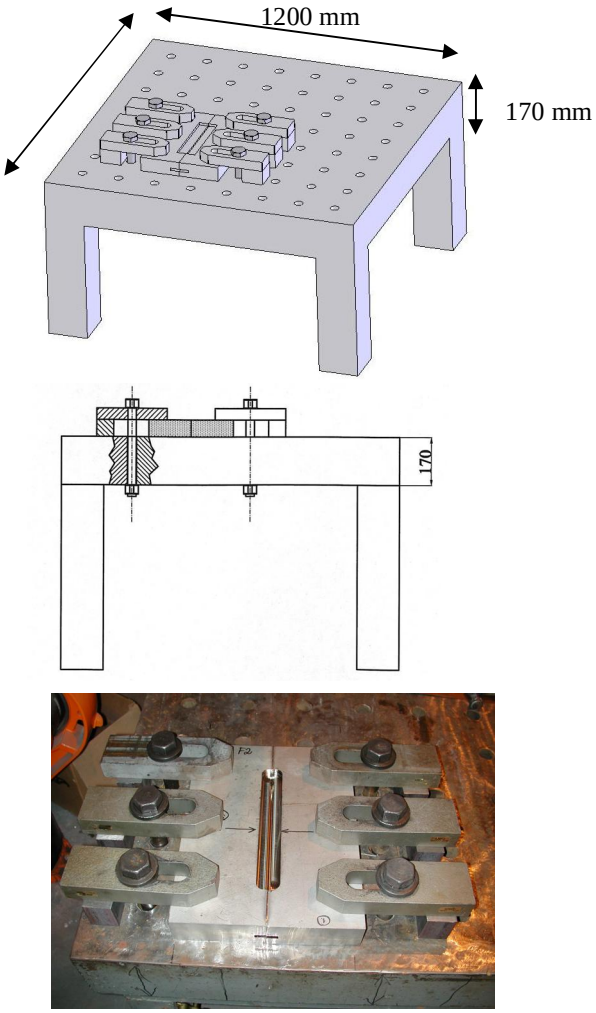

Figure 2. Test set-up for rigid clamping of welded test piece.

Test Pieces

The test piece used was planned to be rigid as it self and to simulate the rigidity of assembly welds. The tested material was AISI 316 L(N)-IG ITER Grade austenitic stainless steel with original thickness of 60 mm. Test piece consisted of two 400 mm x 150 mm plates with thickness of 60 mm. Those 60 mm thick halves were machined in order to posses following features when combined together (Fig. 3): Both ends have close square preparation at the length of 60 mm. The joint thickness, which is intended to be filled using multi pass welds, is 20 mm. The length of the welded joint is 250mm and the joint has a root gap of 1,2 mm.

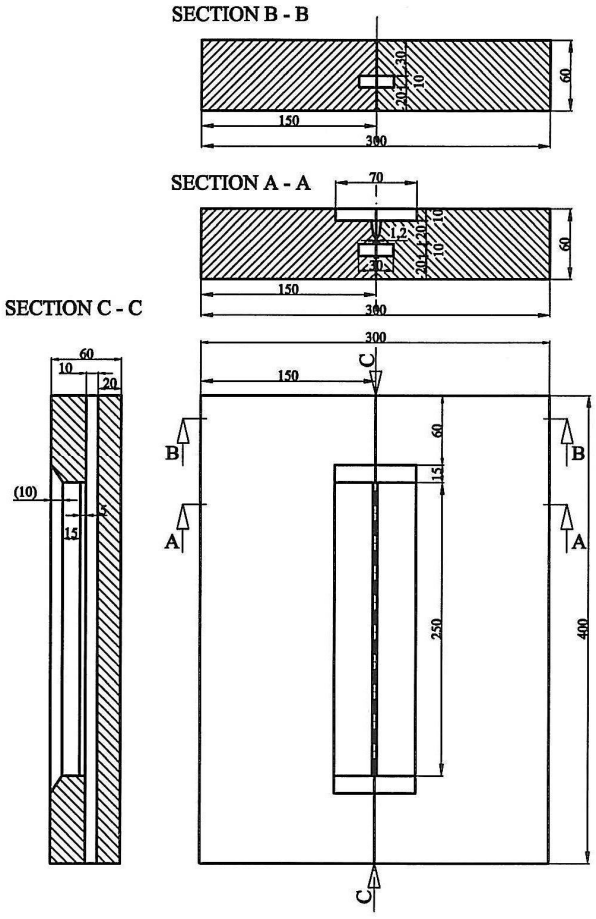

Figure 3. Test piece used in hot cracking tests.

As can be seen in section A-A and C-C in Figure 3, the 20mm thick joint to be welded, is captured near to half way at the whole 60 mm thickness of the test piece. A rectangular cavity for a root of the weld is prepared to be 30 mm x 10 mm. Below the root cavity is a 20 mm thick close square preparation along the whole length of the test piece (400mm).

After machining of necessary groove geometries, two halves were put together and sealed with using electron beam welding at the sections where close square preparations were prepared, Fig. 4. The aim of above mentioned procedure was to prohibit horizontal shrinkage and angular distortions and in that way to produce strains which are correspond to those which can occur in massive components assembly welding.

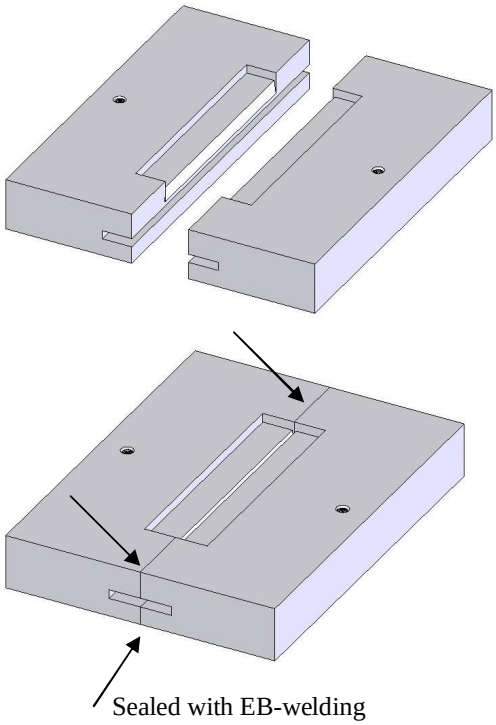

Figure 4. Test piece used in hot cracking tests. Two machined halves are put together and sealed using electron beam welding into the one test piece.

Two kinds of 20 mm thick groove geometries were used in hot cracking tests. The groove geometries are shown in Fig. 5. The basic idea was to use wider (Fig. 5a) and narrower (Fig. 5b) groove configurations, in order to get two different multi pass weld shape together with different depth to width ratios of produced multi pass welds.

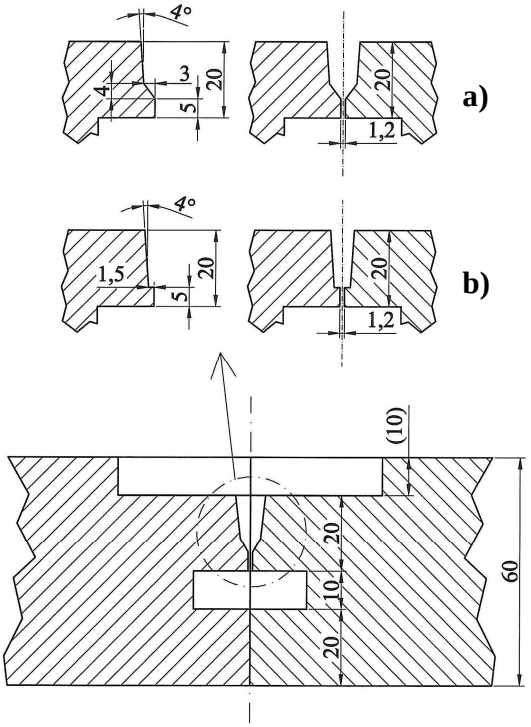

Figure 5. Two different groove geometries were used in hot cracking tests.

Hot Cracking Test Program

As described above, two different groove configurations were decided to use such away that a three copies of test pieces for both groove geometries were prepared. Consequently, we had two test series with three identical hot cracking welding test repetitions in each series. Test pieces with wider groove geometry, Fig. 5a, belonged to the series A and test pieces with narrow groove geometry, Fig. 5b, belonged to the series B. With using preliminary test welding a proper welding parameters were searched for both groove geometries. Thus, both test series had a bit different welding parameters regarding the welding of filling passes, but inside the test series, the same parameters (Table 3. and 4.) were used for welding of each three copies of test pieces.

Before welding experiments, test piece was clamped to the rigid table as described earlier in this paper.

Welding experiments were executed in such away that a keyhole mode hybrid welding was first used in welding of root pass (Fig. 6a) and after that a required amount of filling passes (4…6 passes) were produced with conduction limited hybrid welding. In conduction limited hybrid method, a power density of an Nd:YAG- laser beam spot was purposely dispersed by using strong defocusing (Fig. 6b). Using above procedure, the welding process can be brought inside the conduction limited regime. In addition, a molten filler metal was synergistically added into the laser induced melt pool via a metal inert arc (MIG, Ar + He shielding) welding process. By doing so, a considerable wide melt zones can be produced, which gave a possibility to fill groove gaps which are impossible to fill with using keyhole hybrid welding alone.

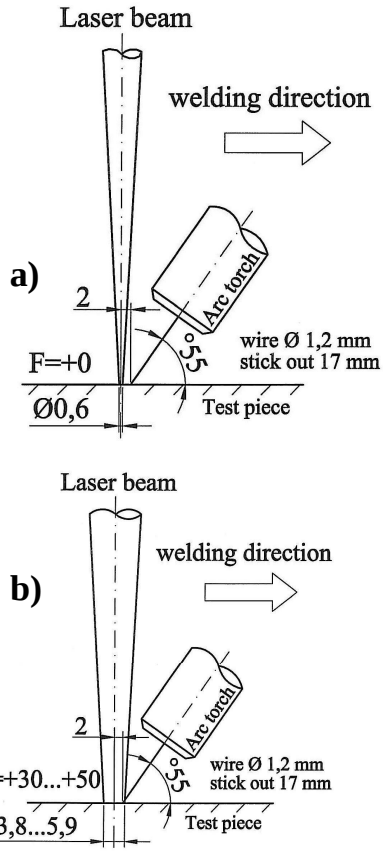

Figure 6. Set-up used in hybrid welding: a) Key-hole mode in welding of root pass and b) Conduction limited mode in welding of filling passes.

Constant welding parameters and variable parameters for the root pass and filling passes can be seen from Table 3 and 4, respectively.

The lay-out of the experimental set-up is shown in Figure 7.

Table 3. Constant welding parameters.

The constant parameters	
Laser power	3 kW
Focal length	200 mm
Horizontal distance between the laser focal point and filler wire feeding point	2 mm
Diameter of filler wire	1,2 mm
Stick out (electrode extension)	17 mm
Orientation and the angle of arc torch	leading, 55°
Shielding gas (MISON He30= Ar+30%He+0,03NO) and flow rate: - Via arc torch's nozzle - Via extra nozzle	 20 l/min 20 l/min

Table 4. Variable welding parameters for the root pass and filling passes.

Welding parameters for the root pass		
Filler wire feeding rate	9,5 m/min (28,8V / 232A)	
Focal point position	± 0mm(spot sizeØ0,6mm)	
Welding speed	1,3 m/min	
Welding parameters for the filling passes		
	Wider groove geometry, Fig.5a **SERIES A**	Narrow groove geometry, Fig.5b **SERIES B**
Filler wire feeding rate	9,0…9,5 m/min (29…30V / 205…260A)	9,0…11 m/min (28…31V / 220…295A)
Focal point position	+50 mm (spot size Ø5,9mm)	+ 30…+40 mm (spot size Ø 3,8…4,9mm)
Welding speed	0,4 m/min	1,0 m/min

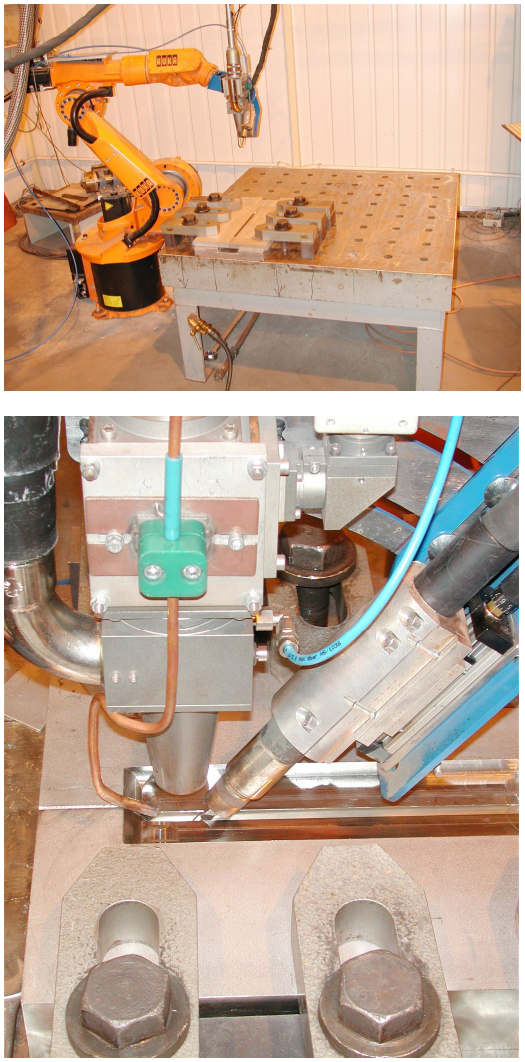

Figure 7. Above: The lay-out of the experimental set-up. Below: Close-up from the hybrid configuration.

After welding, test-pieces were allowed to cool room temperature before clamping was released. Next, test welds were examined by X-ray radiography. After that, test welds were sectioned for macro and micro graphical preparation. Evaluations of the welds were done by the visual inspection from welded test pieces and from the macro and micro graphical cross-sections of the welds and from the X-ray radiographs as well.

Results and Discussion

Multi pass technique was used in hot cracking welding tests. In test welds of series A (wider groove), a total of 5 passes were needed to fill the groove, whereas in test series B (narrow groove), 7 passes were needed. Macrographs from the weld cross-sections of test series A (weld H1, H2 and H3) and test series B (weld H4, H5 and H6) are presented in Figs. 8-13.

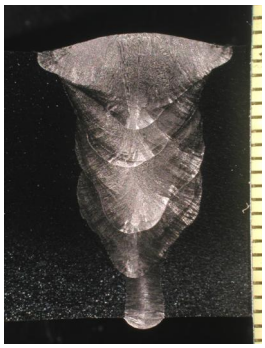

Figure 8. Weld H1 from the test series A.

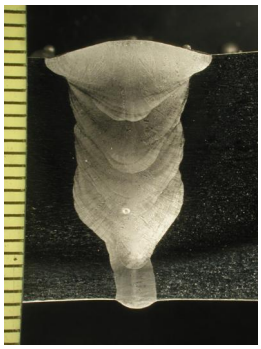

Figure 9. Weld H2 from the test series A.

Figure 9. Weld H3 from the test series A.

Figure 11. Weld H4 from the test series B.

Figure 12. Weld H5 from the test series B.

Figure 13. Weld H6 from the test series B.

During the welding experiments, great attention was paid to the visual inspection of the surface of the intermediate passes. The observations clearly showed that hot cracking, which opened to the surface of the weld pass, did occurred. In test series A, hot cracking occurred only in one test piece of all three: in welding of the first filling pass of multi pass weld H3. In test series B, hot cracking occurred in every test piece. In those test pieces, hot cracking was occurred in the first, second and third filling passes, whereas in root passes no cracking was observed to occur. Under the circumstances, narrow groove configuration used in

series B tented to cause more hot cracking than wider groove configuration used in series A. Observations of hot cracking occurrence in both series are summarized in Table 5 and 6.

Table 5. Occurrence of hot cracking in test series A.

Test series A	Occurrence of hot cracking		
	Weld H1	Weld H2	Weld H3
Root pass	no	no	no
1st filling pass	no	no	**yes**
2nd filling pass	no	no	no
3rd filling pass	no	no	no
4th filling pass	no	no	no

Table 5. Occurrence of hot cracking in test series B.

Test series B	Occurrence of hot cracking		
	Weld H4	Weld H5	Weld H6
Root pass	no	no	no
1st filling pass	**yes**	**yes**	no
2nd filling pass	**yes**	**yes**	**yes**
3rd filling pass	**yes**	**yes**	no
4th filling pass	no	no	no
5th filling pass	no	no	no
6th filling pass	no	no	no

As mentioned earlier, visual evaluation after welding of each filling pass revealed that hot cracks occurred centered at along the weld length and opened to the surface of the weld. In Figure 14a, it is shown an example from the test series B, where the part of the joint was purposely left without upper filling passes in order to authenticate the presence of hot cracking in that case occurring in the first filling pass. In Figure 14b, it is shown the top view from the Figure 14a, which reveals hot cracking opened to the surface of the first filling pass.

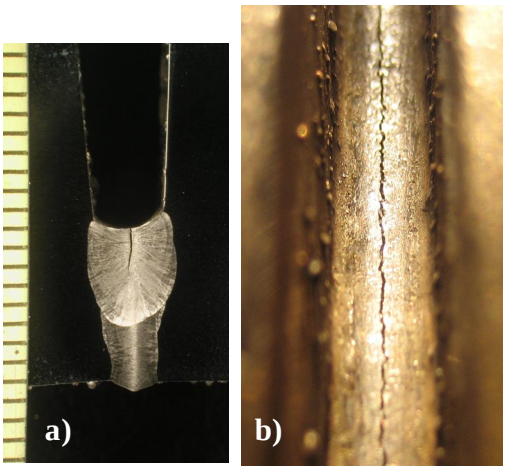

Figure 14. a) Macro cross-section showing hot cracking propagated into the surface of the first filling pass. b) The top view from the Figure 14a showing hot cracking along the weld length.

From the micro graphs presented in Figure 15, it can be seen magnifications (450x) taken from the same cross-section as shown in Figure 14. Micro graphs show the upper and lower part of the hot crack propagated in the fully austenitic microstructure.

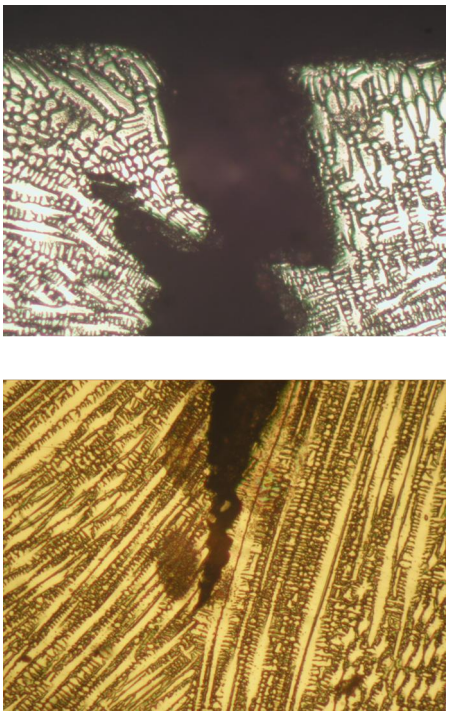

Figure 15. Micro graphs taken from the same cross-section as shown in Figure 14. Micro graphs show the upper and lower part of the hot crack in the fully austenitic microstructure. Magnification 450x.

It seems that during the multi pass welding of this study, the following filling pass has been overlapped into the previous pass such much that molten metal has "healed" the hot crack underneath. Evaluations from the X-ray radiography and from the cross-sectional macro graphs (Figs. 8-13) of the welds seem to support that observation. Anyhow, in general this healing-effect will not be always 100% certain, which must have taken into considerations in production welds of real applications.

In Figures 16a and 16b it is shown weld metal micro structures from the intermediate passes of test weld H3 and H4, respectively. Both weld metals have solidified in primary austenite solidification mode. Fully austenitic microstructure of weld metal is presented in Figures 16a and 16b.

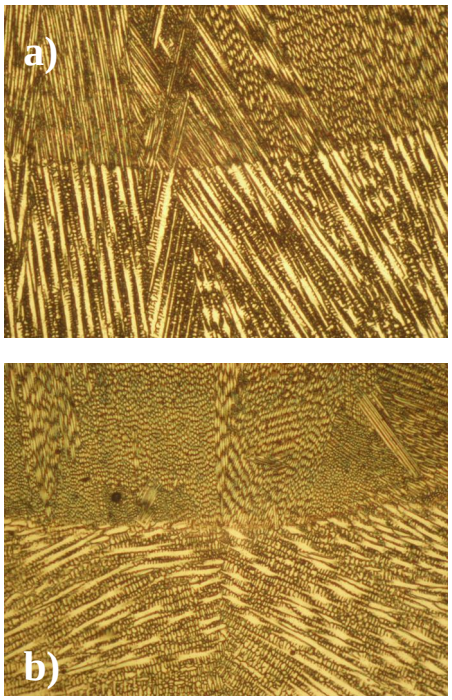

Figure 16. Micro graphs showing fully austenitic microstructure of weld metal in a) test weld H3 and b) H4. Both weld metals have solidified in primary austenite solidification mode. Magnification 230X.

These results are in good agreement with the initial data, as we knew that both parent material and filler wire used, are fully austenitic. In addition, we calculated chromium (Cr_{eq}) and nickel (Ni_{eq}) equivalents of the used parent and filler material using Hammar & Svensson equations: (1) and (2), (Ref. 4)

$$Cr_{eq} = Cr + 1{,}37 \cdot Mo + 1{,}5 \cdot Si + 2 \cdot Nb + 3 \cdot Ti \qquad (1)$$

$$Ni_{eq} = Ni + 0{,}31 \cdot Mn + 22 \cdot C + 14{,}2 \cdot N + Cu \qquad (2)$$

When using the specific chemical compositions given in Table 1 and 2, we had following results:

- Parent material: AISI 316L(N)-IG ITER-grade

$Cr_{eq} = 21{,}47$

$Ni_{eq} = 14{,}33$

$Cr_{eq}/Ni_{eq} = 1{,}50$

- Filler wire material: THERMANIT 19/15

$Cr_{eq} = 24{,}69$

$Ni_{eq} = 20{,}43$

$Cr_{eq}/Ni_{eq} = 1{,}21$

Above Cr_{eq} and Ni_{eq} results are placed in Hammar & Svensson diagram shown in Figure 17.

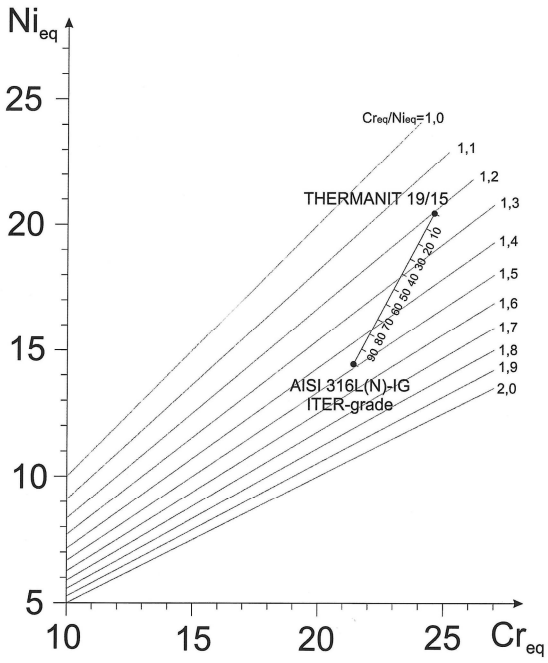

Figure 17. Cr_{eq} and Ni_{eq} values of parent and filler material placed in Hammar & Svensson diagram.

It can be seen from the diagram in Fig. 17, that produced weld metal will follow the segment line starting from point 1,5 and moving along the segment line towards to point 1,2 depending on dilution ratio. Consequently, produced weld metal will have even

smaller Cr_{eq}/Ni_{eq}-ratio than 1.5, because of used filler material.

In the case of this study dilution in filling passes could be in the range of 10…30%, what corresponds roughly Cr_{eq}/Ni_{eq}-ratio of 1,23…1,27 in weld metal. That is way below compared to risk value of 1,5. In that respect, hot cracks in test welds approved that risk according to Cr_{eq}/Ni_{eq}-calculations is for real. One possible to overcome this risk is a correct filler material choice. That is to use more ferritic filler wire material, which will have e.g. a value of Creq/Ni_{eq}-ratio about 2,0 or even higher.

The welded application itself does not necessarily allow 5-15% delta ferrite content in weld metal, because of certain requirements or restrictions. In the case of this study initial requirement was that microstructure of weld metal in joints must be fully austenitic, containing as less as possible delta ferrite at room temperature.

As a whole, results showed that experimental test set-up can produce high strains enough to simulate the conditions which are correspond to those which can occur in massive and rigid components assembly welding. With using test set-up described and with using chosen filler material, hot cracking can be occurred in the rigid AISI 316L(N)-IG ITER steel grade weld joints.

Conclusions

In this study the main objective was to find a method for studying hot cracking susceptibility when a thick section austenitic stainless steel is welded using laser hybrid welding process (3 kW Nd:YAG-laser + GMAW) and multi pass technique. The tested parent material was a specially customized heat: AISI 316L(N)-IG ITER-grade austenitic stainless steel. During this study the test system was first developed and tested. It consisted of a very rigid clamping system and specially designed 60 mm thick test piece which was planned to be rigid as it self.

The results of this study relieved that experimental set-up for rigid clamping can produce high strains enough and hot cracking can be occurred in the rigid AISI 316L(N)-IG ITER steel grade weld joints welded with using multi pass narrow gap laser hybrid welding.

References

[1] Schaeffler, A.L., Met. Progr. 56: 680 and 680B, 1949.

[2] DeLong, W.T. et.al., Weld. J. 35: 526s-532s, 1956.

[3] Hull, F.C., Weld. J. 52: 193s-203s, 1973.

[4] Hammar, Ö. and Svensson, U., Solidification and casting of metals. The Metals Society, London, pp. 401-410, 1979.

[5] Kujanpää, V. et.al., Correlation between solidification cracking and microstructure in austenitic and austenitic-ferritic stainless steel weld, Welding Research International, 9(2):55, 1979.

[6] David, S.A. et. al., Effect of Rapid Solidification on Stainless Steel Weld Metal Microstructures and Its Implications on the Schaeffler Diagram, Weld. J. 66(10): 289s-300s, 1987.

[7] Lippold, J.C., Solidification behaviour and cracking susceptibility of pulsed-laser welds in austenitic stainless steels, Weld. J. 73(6):129s-139s, 1994.

[8] Lippold, J.C., Microstructure Evolution in Austenitic Stainless Steel Laser Welds, Proc. of the Second International Conference on Beam Processing of Advanced Materials, Cleveland, Ohio, USA, pp. 167-178, 1995.

[9] Lienert, T.J., A Combined PSM/Weldability Diagram for Laser Welded Austenitic Stainless Steel, Trends in Welding Research, Proc. of the 5th International Conference, Pine Mountain, Georgia, USA, pp. 724-728, 1998.

[10] Lippold, J.C., Centerline Cracking in Deep Penetration Electron Beam Welds in Type 304L Stainless Steel, Weld. J. 64(5):127s-136s, 1985.